Journal of Magnetic Resonance 194 (2008) 169–174

Contents lists available at ScienceDirect

Journal of Magnetic Resonance

journal homepage: www.elsevier.com/locate/jmr

Improving resolution in single-scan 2D spectroscopy

Philippe Pelupessy [a,*], Luminita Duma [a], Geoffrey Bodenhausen [a,b]

[a] Ecole Normale Supérieure, Département de Chimie, associé au CNRS, 24 rue Lhomond, 75231 Paris Cedex 05, France
[b] Ecole Polytechnique Fédérale de Lausanne, Laboratoire de Résonance Magnétique Biomoléculaire, Batochime, CH-1015 Lausanne, Switzerland

ARTICLE INFO

Article history:
Received 26 May 2008
Revised 26 June 2008
Available online 9 July 2008

Keywords:
NMR
Ultrafast spectroscopy
Aliasing
Undersampling
Band-selective pulses
Bipolar pulsed field gradient pairs

ABSTRACT

New schemes are introduced that allow one to improve the resolution in the indirect dimension of single-scan 'ultrafast' two-dimensional NMR spectra. The methods combine undersampling with band-selective pulses to recover signals that lie outside the detection bandwidth. The efficiency is illustrated for homonuclear total correlation spectroscopy (TOCSY) of quinidine.

1. Introduction

Nuclear magnetic resonance (NMR) spectroscopy has become an essential tool for studying a broad variety of systems and phenomena. Applications range from the search of new drugs to the characterization of internal dynamics of molecules [1]. The advent of two-dimensional (2D) methods made a decisive impact on the evolution of various techniques and greatly contributed to broaden the scope of applications. Traditional two-dimensional experiments are intrinsically time consuming, since many t_1 increments have to be acquired in order to obtain 2D spectra with adequate digital resolution in the indirect ω_1 dimension [2,3], even when samples with sufficient concentration or suitably enhanced nuclear polarization are available. Frydman and co-workers [4,5] have introduced a scheme inspired by echo planar imaging (EPI) [6], enabling the acquisition of a complete 2D NMR spectrum in a single scan, i.e., in less than a second. Thus, the time required to acquire multi-dimensional NMR experiments can be reduced by orders of magnitude. This advantage can be achieved by replacing the usual incrementation of the t_1-evolution interval by a spatial encoding of the phases across the sample, while decoding is performed with the help of alternating gradients applied during the detection period. The spatial encoding can be greatly improved by using adiabatic frequency-modulated pulses [7–9]. This new technique has been successfully combined with liquid chromatography [10] and with methods to increase the polarization of nuclear spins [11]. In addition, the method has been adapted for single-scan magnetic resonance imaging [12,13]. The detection element has been modified to suppress chemical shift evolution in order to obtain J-modulated spectra [14,15].

In contrast to traditional approaches to 2D spectroscopy, the spectral resolution in single-scan experiments is not only limited by the inhomogeneity of the static field and by the homogeneous linewidths that are determined by relaxation, but also by the ability of the decoding gradient to 'unwind' the full spectrum in the indirect dimension. As a result, the spectral widths in the two dimensions are no longer independent of each other: the greater the spectral width that must be covered in either ω_1 or ω_2 dimensions, the poorer the digital resolution in the indirect ω_1 dimension. The present study addresses these limitations by introducing new methods to improve the resolution in the indirect dimension of single-scan multi-dimensional spectra.

2. Theory

We shall briefly sum up the main characteristics of the basic single-scan 2D experiment sketched in Fig. 1 [7]. Effects of relaxation and of inhomogeneous fields will be neglected. The sequence starts with the excitation of spin S followed by frequency encoding using two consecutive adiabatic pulses each of duration τ_E with a linear sweep of the radio-frequency (RF) carrier over a range $\Delta\, \nu_{ad}$. These two adiabatic encoding pulses are applied in the presence of two pulsed field gradients (PFGs) with the same strength $\boldsymbol{g}_E(\boldsymbol{r})$ but with opposite signs, in the manner of 'bipolar pulse pairs'. The phase ϕ_E of the coherence of a spin S after frequency encoding depends on the position $\boldsymbol{r}$ of spin S in the sample:

* Corresponding author. Fax: +33 1 44 32 33 97.
E-mail address: philippe.pelupessy@ens.fr (P. Pelupessy).

1090-7807/$ - see front matter © 2008 Elsevier Inc. All rights reserved.
doi:10.1016/j.jmr.2008.06.023

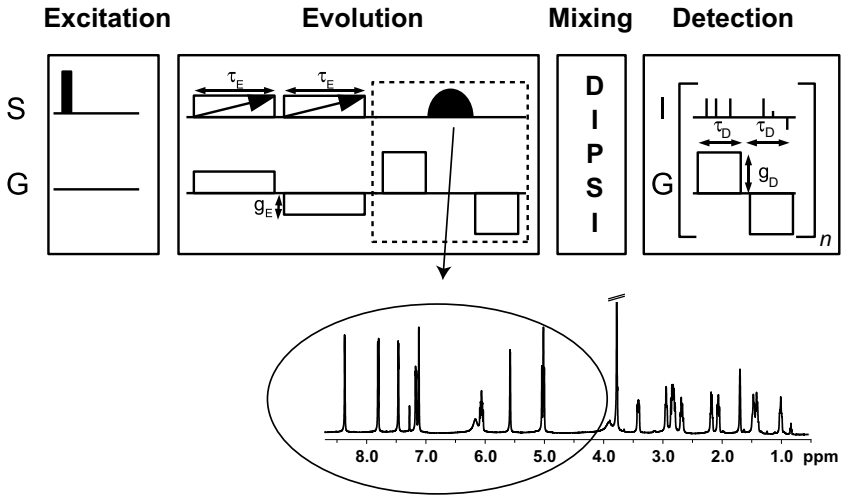

Fig. 1. Basic scheme for single-scan 2D experiments. The experiment starts with the excitation of S spin coherence by a $\pi/2$ pulse, which can be replaced by another preparation sequence such as INEPT. A pair of adiabatic pulses with linear frequency sweeps combined with a bipolar pulsed gradient pair results in the encoding of the desired phase profile. A suitable mixing sequence (the sketch shows a DIPSI sequence appropriate for TOCSY) leads to a transfer of coherence from spin S to I. The acquisition occurs during a train of alternating decoding gradients. In the example of quinidine shown below, the basic range between 0 and 4.5 ppm of the spectrum is observed directly in each τ_D interval, but the circled part between 4.5 and 9 ppm lies outside the observed range. The element in the dashed box, comprising a bipolar pulse pair with a frequency-band-selective refocusing pulse (BPP-BSRP) has the effect of shifting the signals in the circled part of the spectrum into the observable range, thus leading to the recovery of this part of the spectrum (see Figs. 4 and 5). If the band-selective π pulse is phase-shifted through x, y in the manner of EXORCYCLE [18], the sum of the signals corresponds to the part of the spectrum that is not affected by the π pulse, while the difference gives the region which is refocused.

$$\phi_E = -\{4\tau_E/(2\pi\Delta\nu_{ad})\}\Omega_S\gamma_S\boldsymbol{g}_E(\boldsymbol{r})\cdot\boldsymbol{r} \tag{1}$$

where γ_S is the gyro-magnetic ratio of spin S, and Ω_S its chemical shift with respect to the RF carrier in the center of the sweeps. We shall henceforth assume that the gradient is applied along the z-axis, and hence replace $\boldsymbol{r}$ by z and $\boldsymbol{g}_E$ by g_E. After the encoding period, the coherence can be transferred from spin S to spin I during a suitable mixing interval. The example of Fig. 1 shows a DIPSI (Decoupling In the Presence of Scalar Interactions) [16] sequence for total correlation spectroscopy (TOCSY) [17]. If we define t_1 to be the time running from the beginning of each positive lobe of the alternating decoding gradients, τ_D as the duration of each decoding gradient, and n as the counter of the decoding gradient pair (each pair having a duration $2\tau_D$), we can define a running variable $t_2 = 2n\,\tau_D$, so that the signal acquired during the positive lobes of the alternating gradients of amplitude g_D is given by

$$s(z,t_1,n) = NP_{S,I}\exp[\mathrm{i}\phi_E + \mathrm{i}\gamma_I g_D z t_1 + i\Omega_I(t_1+t_2)] \tag{2}$$

where N is a normalization factor, and $P_{S,I}$ is the probability that coherence transfer occurs from spin S to I. If this transfer is associated with a phase-shift, $P_{I,S}$ may be a complex number. When normalizing the initial amplitude to one and integrating over the effective sample height h, one obtains the total signal:

$$s(t_1,t_2) = P_{S,I}\mathrm{sinc}(-\alpha\Omega_S + \beta t_1)\exp[\mathrm{i}\Omega_I(t_1+t_2)] \tag{3}$$

where $\alpha = \tau_E\gamma_S g_E h/(\pi\Delta\nu_{ad})$ and $\beta = \gamma_I g_D h/2$. The signals acquired during the negative lobes of the detection gradient pairs are mirror images of the ones recorded during the positive lobes, apart from a phase factor which depends on Ω_I.

In traditional two-dimensional experiments, the digital resolution, i.e., the separation $\Delta\nu_i$ between neighboring points in the digitized spectra in the indirect $\nu_1 = \omega_1/(2\pi)$ dimension ($i = 1$) and in the direct $\nu_2 = \omega_2/(2\pi)$ dimension ($i = 2$) is determined by the corresponding acquisition times:

$$\Delta\nu_i = 1/(N_i\Delta\mathrm{t}_i) = 1/t_i^{\max} \tag{4}$$

where N_i is the number of acquisition points, Δt_i the increment, and $t_i^{\max}$ the acquisition time. For a given spectral width, which is inversely proportional to Δt_i, the digital resolution can always be improved by increasing the number N_i of observed data points. Thus, the digital resolution parameters $\Delta\nu_1$ and $\Delta\nu_2$ in the two dimensions of traditional 2D spectra are independent of each other. An improved resolution in the indirect dimension requires a longer experimental time.

This tenet no longer holds in single-scan experiments. In the direct ω_2 dimension, Eq. (4) is still valid, but there is no equivalent in the indirect ω_1 dimension of single-scan experiments, since no Fourier transformation is performed. Therefore, to compare experiments, we have to use another definition of the resolution. In a traditional 2D experiment, the shape of a peak $s(\nu)$ that is centered at a frequency ν_I and results from the Fourier transformation of a truncated time-domain signal can be approximately described by:

$$s_i(\nu) = \mathrm{sinc}[2\pi(\nu-\nu_I)t_i^{\max}] \tag{5}$$

We can define the spectral resolution as the interval between the maximum and the first zero passage of this sinc function:

$$\Delta\nu_i = 1/(2t_i^{\max}) \tag{6}$$

For single-scan experiments, Eq. (3) describes a lineshape that is similar to Eq. (5) for conventional Fourier transform spectra. By analogy to Eq. (6), bearing in mind that the peaks appear at different points of time in the τ_D interval of single-scan experiments, we can define

$$\Delta t_1 = 2\pi/\gamma_I g_D h = 1/\Delta\nu_D^I \tag{7}$$

where Δt_1 stands for the interval between the maximum and the first zero passage of Eq. (3), and $\Delta\nu_D^I$ is the frequency range that the decoding gradients g_D impose on the I spins. It is remarkable that the temporal resolution does *not* depend on the parameters of the initial encoding sequence. The lineshape in the indirect dimension is identical to that of a gradient echo. The linewidth is determined by the effective sample height h and the strength g_D of the decoding gradient, while the position of the echo depends on the chemical shift Ω_S of spin S. In units of frequency, the spectral resolution $\Delta\nu_1$ in the indirect domain is given by

$$\Delta\nu_1 = W_1\Delta t_1/\tau_D \tag{8}$$

where the spectral width W_1 in the indirect dimension can be deduced from Eq. (3):

$$W_1 = \tau_D \beta/\alpha = \tau_D \gamma_I g_D \pi \Delta\nu_{ad}/(2\tau_E \gamma_S g_E) \quad (9)$$

The duration τ_D of each decoding gradient corresponds to half the dwell time Δt_2 in the direct dimension, hence:

$$\Delta\nu_1 = 2W_1/(\Delta t_2 \Delta\nu_D^I) = 2W_1 W_2/\Delta\nu_D^I \quad (10)$$

The full width at half height, which is easy to determine experimentally, is related to $\Delta\nu_1$ as follows [15]:

$$\Delta\nu_1^{FWHH} = 1.21\Delta\nu_1 \quad (11)$$

Thus, the spectral resolution $\Delta\nu_1$ in the indirect dimension depends on the strength of the decoding gradients and on the spectral widths in *both* indirect and direct dimensions. The greater the spectral width that needs to be covered in *either* dimension, the worse the spectral resolution in the indirect dimension. The development of strong pulsed field gradients with short switching delays and appropriately sturdy probes will therefore be crucial for improving the spectral quality in single-scan multi-dimensional experiments. However, very intense gradients may lead to signal losses because of translational diffusion [19,20]. The spectral resolution in the indirect dimension, when expressed in ppm, is proportional to the strength of the static magnetic field. Thus, at higher B_0 fields, the resolution in the indirect dimension will be degraded. Note that an increase of the amplitude of the decoding gradients alone is not enough to improve the spectral resolution in the indirect dimension. Although the peaks will be sharper, they will be spread over a smaller time span because a larger spectral width W_1 is covered. If one covers the full spectral width with a given strength of the decoding gradient, increasing this gradient strength will merely add empty regions to the spectrum. In order to improve the resolution, the other parameters of Eq. (9) need to be adapted to restore the desired spectral width, W_1. For *fixed* spectral widths W_1 and W_2, the resolution in the indirect dimension improves with increasing decoding gradient strengths. Hereafter, we explore avenues to improve the resolution in the indirect dimension when the limits of the decoding gradients are attained.

In Fig. 2a, the poor spectral resolution is illustrated for a 500 mM sample of quinidine in deuterated chloroform recorded at 295 K. The experiment of Fig. 1 was carried out without mixing sequence (so that only signals along the diagonal of the two-dimensional spectra are expected) in a static field $B_0 = 14.1$ T (600 MHz for protons). The excitation element contains two consecutive adiabatic WURST (Wideband Uniform Rate and Smooth Truncation) [21] pulses applied in the presence of two PFGs with the same strength but opposite signs. Both PFGs were applied along the *x* and *z* directions. The use of additional gradients along the *x*-axis does not change the resolution significantly but reduces the 'sinc wiggles' of the signals [22]. Each adiabatic encoding pulse had a duration $\tau_E = 6$ ms with a linear sweep of the RF carrier over a range $\Delta\nu_{ad} = 40$ kHz. In the direct dimension, a dwell-time $\Delta t_2 = 2\tau_D = 208$ μs is required to cover the full width of the proton spectrum of 4.8 kHz width (8 ppm). This merely leaves $\tau_D = 104$ μs for each lobe of the alternating decoding gradients in the acquisition interval. A total of $n = 512$ gradient pairs with a sinusoidal smoothing of the initial and final 20 μs [23] amplitude profile of ca. 11 G/cm, i.e., 20% of the maximum strength, have been used during signal acquisition which lasted about 106 ms. A home-written program taking into account the smoothness of the amplitude profile, the number of gradient echoes and the duration of each decoding gradient was used to optimize the decoding pulse gradients. The resolution in the indirect dimension is inadequate for most practical purposes.

Since the maximum allowed strength g_D of the decoding gradients is necessarily limited, the best way to increase the spectral resolution in the indirect dimension is to increase the duration τ_D of the decoding gradients. Unfortunately, this leads to a decrease of the spectral width in the direct ω_2 dimension. In Fig. 2b and c the dwell-time $\Delta t_2 = 2\tau_D$ was first doubled and then quadrupled with respect to Fig. 2a. This corresponds to detection gradients of 208 and 416 μs, respectively (both with a sinusoidal smoothing of the initial and final 20 μs). Of course, the spectrum in the indirect ω_1 dimension has to be "spread out" at the same time. This can be achieved either by prolonging the duration τ_E of the encoding gradients and concomitant adiabatic pulses, or by increasing the amplitudes of the encoding gradients. The latter solution is only possible if the sweep width of the adiabatic encoding pulses adequately covers the frequency range imposed on the *S* spins by the gradients. If losses due to transverse relaxation, scalar couplings or diffusion during the encoding interval are significant, it is important to reduce the frequency range of the adiabatic pulse as much as possible [7,15,24] and only a prolongation of the encoding gradients is feasible. Note that in our experiments the total length of the encoding period was only 12 ms so that the frequency range of the adiabatic pulse could safely be chosen large enough to absorb increases in the amplitude of the encoding gradient. The gain in resolution in the indirect ω_1 dimension is evident. The peaks that lie outside the spectral width in the direct ω_2 dimension are simply aliased in. For a sample height of 1.6 cm, the theoretical

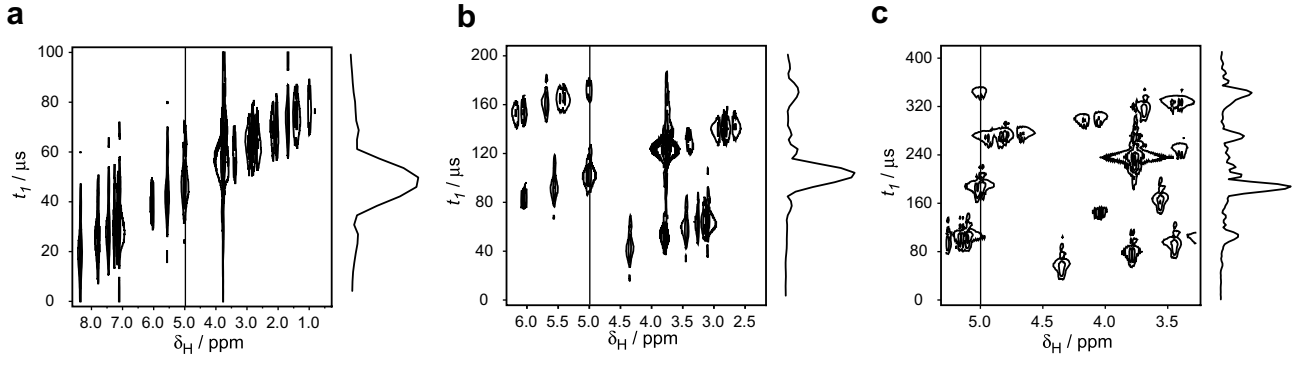

Fig. 2. Single-scan 2D proton spectra of quinidine in $CDCl_3$ using the experiment described in Fig. 1 without mixing period (diagonal peaks only). On the right side of each spectrum, a column extracted at $\omega_2 = 5$ ppm is shown. The amplitude of the encoding gradients applied along *x* and *z* directions was ca. (a) 0.25 G/cm, (b) 0.55 G/cm and (c) 1.21 G/cm while the amplitude of the decoding gradients was 11 G/cm for all experiments. The duration of the decoding gradients was increased from (a) $\tau_D = 104$ μs to (b) 208 μs and (c) 416 μs. The longer τ_D, the better the resolution in the vertical indirect dimension. However, the spectral width in the horizontal direct ω_2 dimension is inversely proportional to τ_D, since the dwell time (interval between sampling points) is $\Delta t_2 = 2\tau_D$. The spectral width in the ω_2 dimension is thus reduced from (a) 4.8 kHz (8.01 ppm) to (b) 2.4 kHz (4.01 ppm) and (c) 1.2 kHz (2.00 ppm). Consequently, peaks that lie outside the spectral width are aliased in the direct ω_2 dimension.

full width at half height of the signals in the indirect dimension, as can be deduced from Eqs. (10) and (11), is 16.1 μs. The widths at half height of the resonance at 5 ppm in Fig. 2a–c were 16.8 ± 1.0, 17 ± 1.0 and 17.2 ± 1.0 μs, corresponding to 2.12, 0.95 and 0.43 ppm. The gains in resolution are better than would be expected from doubling or quadrupling the decoding gradient amplitudes. This can be explained by the fact that the transition period between the positive and negative decoding gradients (always maintained at 40 μs) takes percentage-wise less time when the duration of the decoding gradients increases.

The spectra in Fig. 3a and b were obtained with the same parameters as Fig. 2a and c, except that a DIPSI-2 mixing sequence of 22 ms duration was inserted (see Fig. 1) to bring about a transfer of coherence between all spins in the manner of TOCSY.

If the one-dimensional proton spectrum is known, the original positions of the peaks can easily be reconstructed. Powerful methods exist to choose a spectral width that is as small as possible without generating any ambiguities due to folding [25–27]. If the proton spectrum is unknown, one should repeat the experiment with a slightly different spectral width in the direct ω_2 dimension. Peaks that are aliased move as shown in Fig. 3c. The price to pay for this method is a loss in sensitivity. The signal-to-noise ratio is inversely proportional to the square root of the dwell time $2\tau_D$, since fewer points are acquired in the direct dimension if $2\tau_D$ is increased. Like the signals, the noise is aliased into the reduced observable spectral width. Note that extending the duration of the decoding gradient while decreasing its amplitude does not reduce diffusion losses [15]. Hence, to obtain an optimum spectral resolution, one should always choose an amplitude that is as high as safely possible before increasing the duration.

Another way to improve the resolution would be to compromise on the spectral width in the indirect ω_1 dimension. According to Eq. (10), the smaller the spectral width W_1, the better the spectral resolution. In Fig. 4a, half of the spectrum of Fig. 2a has been "cut away" in order to increase the resolution. In order to recover the missing part of the spectrum, the experiment could be repeated after shifting the carrier frequency to the center of this part. A more efficient approach uses a band-selective refocusing pulse (BSRP) to recover the missing part of the spectrum. This π pulse must be flanked by a bipolar pulse pair (BPP) comprising two gradients, as shown in the dashed box in Fig. 1. This gradient pair shifts the apparent frequencies of the spins that are refocused (circled resonances in Fig. 1) while it does not affect the region that is not touched by the pulse. By fine-tuning the parameters of the gradients, the missing part of the spectrum can be shifted at will. Fig. 4b shows the effect of such a manipulation. Since a single π pulse is applied, the peaks that are recovered appear along an "anti-diagonal". By shifting the phase of the band-selective pulse through 90°, in the manner of EXORCYCLE [18], the folded peaks change their sign. Thus, the sum of the spectra in Fig. 4c gives the original spectrum of Fig. 4a, while the difference in Fig. 4d gives the missing part. An advantage of this method is that it does not lead to a loss in signal-to-noise, apart from minor losses induced by relaxation during the band-selective pulse. If two separate experiments are carried out with a phase shift, the signal-to-noise increases with each scan, like in Hadamard spectroscopy [28]. This method is particularly advantageous when there are empty regions in the spectrum and could be generalized to shift more than one region by applying multiple BPP-BSRP elements.

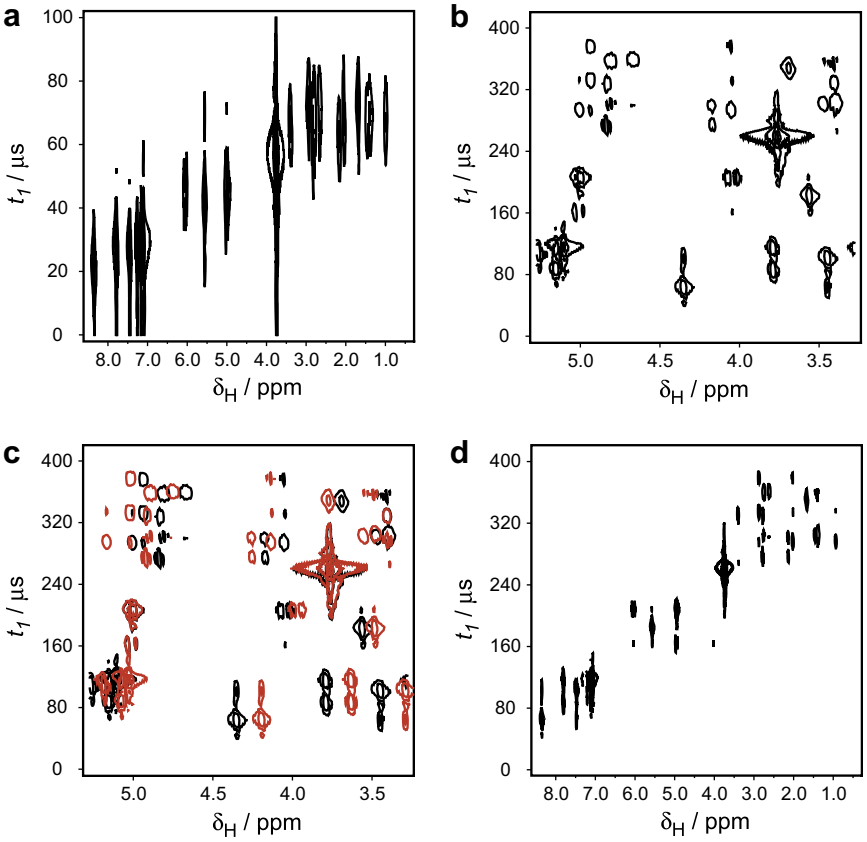

Fig. 3. Single-scan 2D TOCSY spectra of quinidine. Spectra (a) and (b) were recorded with the same parameters as in Fig. 2a and c, except for the insertion of a DIPSI-2 mixing sequence. The red peaks in (c) were obtained by reducing the length of the decoding gradient from τ_D = 416 μs to 400 μs, all other parameters being identical as in Fig. 2b. The black signals in (b), obtained with τ_D = 416 μs, were superimposed on top of the red signals in (c). The spectral widths corresponding to the red and black signals are 2.08 ppm and 2.00 ppm, respectively. The red peaks that are shifted by ±0.08 ppm are aliased once in the horizontal direct ω_2 dimension, while those that are shifted by ±0.16 ppm are aliased twice. (d) Un-aliased TOCSY spectrum reconstructed from (c).

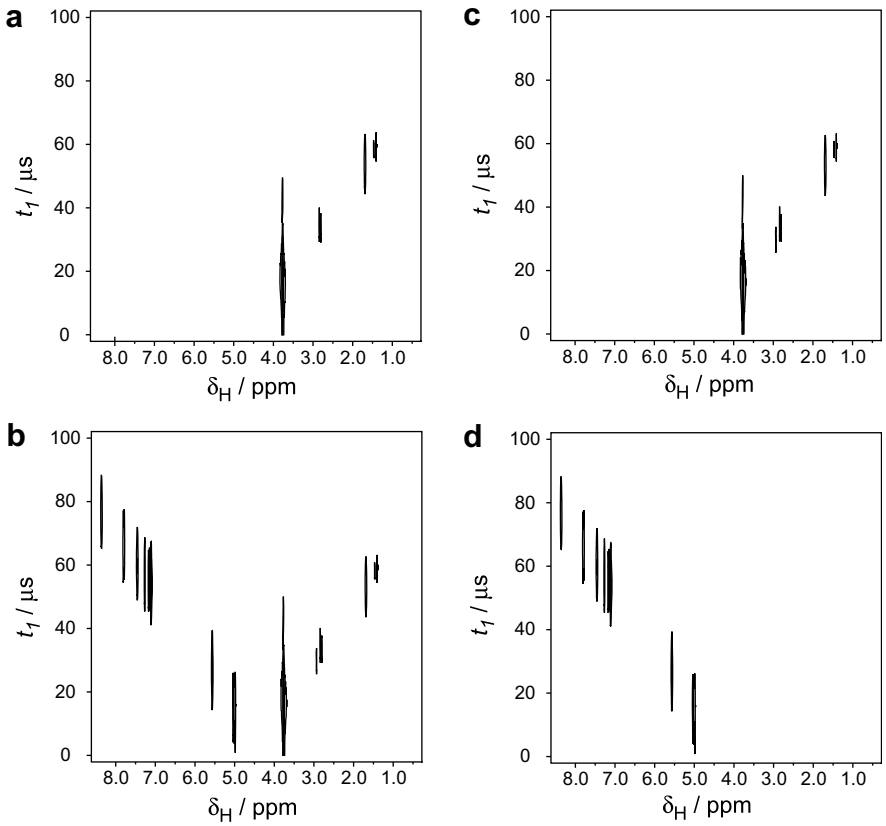

Fig. 4. Single-scan 2D spectra without mixing interval (diagonal peaks only). The parameters are chosen in such a way that only half of the spectrum fits in the spectral width of the vertical indirect ω_1 dimension. Compared to Fig. 2a, the resolution in this dimension is enhanced. (b) To recover the missing peaks, a BPP-BSRP element comprising a band-selective π pulse flanked by two gradients of opposite sign has been inserted (see Fig. 1). The experiment has been repeated with a 90° phase shift of the band-selective π pulse (not shown). (c) The sum of the two experiments gives the initially selected region while (d) the difference results in the peaks that are missing in (a).

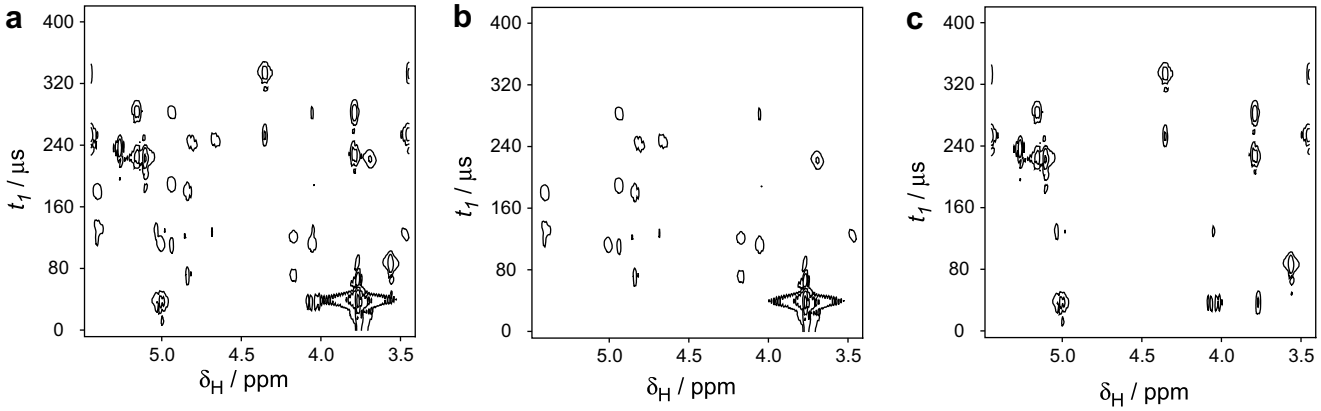

Fig. 5. Single-scan TOCSY spectra of quinidine. In order to maximize the resolution in the indirect dimension, the two methods described in the text have been combined; a spectral width of only 1.2 kHz (2 ppm at 600 MHz) is used in the direct ω_2 dimension and only half of the full spectrum fits in the observable window in the indirect ω_1 dimension, the remaining part being "recovered" by the band-selective pulses shown in Fig. 1. Fig. 5a–c are equivalent to Fig. 4b–d.

The two ways of improving the resolution presented in this work can be combined, i.e., the prolongation of the duration of the decoding gradients τ_D, and the recovery of a missing part of the spectrum by a BPP-BSRP element. This is shown in Fig. 5a–c.

3. Conclusions

The spectral resolution in the indirect ω_1 dimension of single-scan multi-dimensional experiments can be improved by increasing the strength of the alternating decoding gradients in the acquisition interval while keeping the same spectral width in both dimensions. In practice however, the gradient strength is limited for technical reasons and translational diffusion may cause signal losses if the gradients are too strong. Another approach is to limit the spectral width in the indirect dimension by using stronger and/or longer encoding gradients. Band-selective refocusing pulses flanked by a bipolar pulse pair of gradients (a so-called BPP-BSRP element) can then recover peaks that lie outside the detectable spectral width in the indirect dimension. As an alternative, the dwell time in the direct ω_2 dimension can be prolonged to make room for longer decoding gradients. This leads to a narrower spectral width in the direct dimension, and hence to aliasing, but no

signals are lost. The two methods can be combined in order to further improve the digital resolution.

Acknowledgments

The authors are indebted to the Centre National de la Recherche Scientifique (CNRS, France), the Agence Nationale pour la Recherche (ANR, France), the Integrated Infrastructure Initiative (I3) of the 6th Framework Program of the EC (Contract # RII3-026145, EU-NMR), the Fonds National de la Recherche Scientifique (FNRS, Switzerland), and the Commission pour la Technologie et l'Innovation (CTI, Switzerland).

References

[1] D.M. Grant, R.K. Harris (Eds.), Encyclopedia of Nuclear of Magnetic Resonance, John Wiley & Sons Ltd., Chichester, 1996.
[2] J. Jeener, Lecture at International Ampère Summer School, Basko Polje, Yugoslavia, 1971.
[3] W.P. Aue, E. Bartholdi, R.R. Ernst, 2-Dimensional spectroscopy—application to nuclear magnetic resonance, J. Chem. Phys. 64 (1976) 2229–2246.
[4] L. Frydman, T. Scherf, A. Lupulescu, The acquisition of multidimensional NMR spectra within a single scan, Proc. Natl. Acad. Sci. USA 99 (2002) 15858–15862.
[5] L. Frydman, A. Lupulescu, T. Scherf, Principles and features of single-scan two-dimensional NMR spectroscopy, J. Am. Chem. Soc. 125 (2003) 9204–9217.
[6] M.K. Stehling, R. Turner, P. Mansfield, Echo-planar imaging—magnetic-resonance-imaging in a fraction of a second, Science 254 (1991) 43–50.
[7] P. Pelupessy, Adiabatic single scan two-dimensional NMR spectroscopy, J. Am. Chem. Soc. 125 (2003) 12345–12350.
[8] N.S. Andersen, W. Kockenberger, A simple approach for phase-modulated single-scan 2D NMR spectroscopy, Magn. Reson. Chem. 43 (2005) 795–797.
[9] A. Tal, B. Shapira, L. Frydman, A continuous phase-modulated approach to spatial encoding in ultrafast 2D NMR spectroscopy, J. Magn. Reson. 176 (2005) 107–114.
[10] B. Shapira, A. Karton, D. Aronzon, L. Frydman, Real-time 2D NMR identification of analytes undergoing continuous chromatographic separation, J. Am. Chem. Soc. 126 (2004) 1262–1265.
[11] L. Frydman, D. Blazina, Ultrafast two-dimensional nuclear magnetic resonance spectroscopy of hyperpolarized solutions, Nat. Phys. 3 (2007) 415–419.
[12] Y. Shrot, L. Frydman, Spatially encoded NMR and the acquisition of 2D magnetic resonance images within a single scan, J. Magn. Reson. 172 (2005) 179–190.
[13] A. Tal, L. Frydman, Spectroscopic imaging from spatially-encoded single-scan multidimensional MRI data, J. Magn. Reson. 189 (2007) 46–58.
[14] P. Giraudeau, S. Akoka, A new detection scheme for ultrafast 2D J-resolved spectroscopy, J. Magn. Reson. 186 (2007) 352–357.
[15] P. Giraudeau, S. Akoka, Resolution and sensitivity aspects of ultrafast J-resolved 2D NMR spectra, J. Magn. Reson. 190 (2008) 339–345.
[16] L. Braunschweiler, R.R. Ernst, Coherence transfer by isotropic mixing—application to proton correlation spectroscopy, J. Magn. Reson. 53 (1983) 521–528.
[17] A.J. Shaka, C.J. Lee, A. Pines, Iterative schemes for bilinear operators—application to spin decoupling, J. Magn. Reson. 77 (1988) 274–293.
[18] G. Bodenhausen, R. Freeman, D.L. Turner, Suppression of artifacts in 2-dimensional J-spectroscopy, J. Magn. Reson. 27 (1977) 511–514.
[19] P. Giraudeau, S. Akoka, Sources of sensitivity losses in ultrafast 2D NMR, J. Magn. Reson. 192 (2008) 151–158.
[20] Y. Shrot, L. Frydman, The effects of molecular diffusion in ultrafast two-dimensional nuclear magnetic resonance, J. Chem. Phys. 128 (2008) 15.
[21] E. Kupce, R. Freeman, Adiabatic pulses for wide-band inversion and broad-band decoupling, J. Magn. Reson. Ser. A 115 (1995) 273–276.
[22] K.E. Cano, M.J. Thrippleton, J. Keeler, A.J. Shaka, Cascaded z-filters for efficient single-scan suppression of zero-quantum coherence, J. Magn. Reson. 167 (2004) 291–297.
[23] J.M. Böhlen, G. Bodenhausen, Experimental aspects of Chirp NMR-spectroscopy, J. Magn. Reson. Ser. A 102 (1993) 293–301.
[24] B. Shapira, Y. Shrot, L. Frydman, Symmetric spatial encoding in ultrafast 2D NMR spectroscopy, J. Magn. Reson. 178 (2006) 33–41.
[25] D. Jeannerat, High resolution in heteronuclear H-1-C-13 NMR experiments by optimizing spectral aliasing with one-dimensional carbon data, Magn. Reson. Chem. 41 (2003) 3–17.
[26] D. Jeannerat, Computer optimized spectral aliasing in the indirect dimension of H-1-C-13 heteronuclear 2D NMR experiments. A new algorithm and examples of applications to small molecules, J. Magn. Reson. 186 (2007) 112–122.
[27] E. Lescop, P. Schanda, R. Rasia, B. Brutscher, Automated spectral compression for fast multidimensional NMR and increased time resolution in real-time NMR spectroscopy, J. Am. Chem. Soc. 129 (2007) 2756–2757.
[28] E. Kupče, T. Nishida, R. Freeman, Hadamard NMR spectroscopy, Prog. NMR Spectrosc. 42 (2003) 95–122.